Monte Carlo Simulations of Spin Glasses at Low Temperatures

Helmut G. Katzgraber, Matteo Palassini and A. P. Young
Department of Physics, University of California, Santa Cruz, CA 95064
(January 29, 2001)

We report the results of Monte Carlo simulations on several spin glass models at low temperatures. By using the parallel tempering (Exchange Monte Carlo) technique we are able to equilibrate down to low temperatures, for moderate sizes, and hence the data should not be affected by critical fluctuations. Our results for short range models are consistent with a picture proposed earlier that there are large scale excitations which cost only a finite energy in the thermodynamic limit, and these excitations have a surface whose fractal dimension is less than the space dimension. For the infinite range Viana-Bray model, our results obtained for a similar number of spins are consistent with standard replica symmetry breaking.

PACS numbers: 75.50.Lk, 75.40.Mg, 05.50.+q

I. INTRODUCTION

There has recently been a renewed interest in the nature of the spin glass phase. Two principal theories have been investigated: the "droplet model" proposed by Fisher and Huse[1], (see also Refs. 2, 3), and the replica symmetry breaking (RSB) picture of Parisi[4–6]. These scenarios and some others have also been considered by Newman and Stein[7]. An important difference between these models concerns the number of large-scale, low energy excitations. RSB theory follows the exact solution of the infinite range Sherrington-Kirkpatrick (SK) model in predicting that there are excitations which involve turning over a finite fraction of the spins and which cost only a *finite* amount of energy in the thermodynamic limit. In addition, the surface of these large, finite energy excitations is expected[8] to be space filling which means that the fractal dimension of their surface, d_s, is equal to the space dimension, d. The droplet theory argues that the lowest energy excitation involving a given spin and which has linear spatial extent L typically costs an energy L^{θ}, where θ is a (positive) exponent. Hence, in the thermodynamic limit, excitations which flip a finite fraction of the spins cost an *infinite* amount of energy. The droplet theory also predicts that $d_s < d$.

Recently, Krzakala and Martin[9] (KM), and two of us[10] (PY), have argued that a straightforward interpretation of their numerical results at zero temperature is intermediate between the droplet and RSB pictures in that there appear to be large scale excitations whose energy does not increase with size, but these have a surface with $d_s < d$. This interpretation of the results of KM and PY has, however, been recently challenged (though in opposite senses) by Marinari and Parisi[11] and by Middleton[12]. There has also been recent debate[13–16] as to whether the $\pm J$ model has similar behavior to that of a model with a continuous distribution. In the scenario of KM and PY it is necessary to introduce *two* exponents which describe the growth of the energy of an excitation of scale L: (i) θ (> 0) such that L^{θ} is the typical change in energy when the boundary conditions are changed, for example from periodic to anti-periodic, and (ii) θ', which characterizes the energy of clusters excited within the system for a *fixed* set of boundary conditions. In this paper we test whether the picture proposed by KM and PY is compatible with finite temperature Monte Carlo simulations.

Several previous Monte Carlo simulations[17–19,8] have found evidence for finite energy large scale excitations by looking at the order parameter function $P(q)$. In the thermodynamic limit this has delta functions at (plus or minus) the Edwards-Anderson order parameter, q_{EA}, corresponding to ordering within a single valley, and, according to RSB theory, a tail with a finite weight extending down to $q = 0$. In the droplet theory, $P(q)$ is trivial, i.e. has only delta functions at $\pm q_{EA}$, though in a finite system there is a weight at the origin which vanishes with increasing L like[1] $L^{-\theta}$.

These earlier Monte Carlo studies have found that the weight of $P(q)$ at the origin is independent of the systems size for temperatures down to $T \simeq 0.7\, T_c$ in three dimensions[18] and $T \simeq 0.6\, T_c$ in four dimensions[19]. However, these studies have been criticized[20,21] as being too close to the critical point, so that the results are affected by critical fluctuations and very much larger sizes would be needed at these temperatures to see the asymptotic behavior of the low-temperature spin-glass state[22]. Refs. 20, 21 also argue, however, that clear evidence for droplet theory behavior could be seen even for quite small sizes at *very* low temperatures.

In this paper we check this prediction by performing Monte Carlo simulations in the low temperature region, though with an admittedly modest range of sizes, using the "parallel tempering" Monte Carlo method[23,24], also known as Exchange Monte Carlo. One difficulty with this approach is to ensure equilibration since the technique proposed earlier by one of us and Bhatt[25] for conventional Monte Carlo does not work for parallel tempering. Here we use an alternative method, valid for the important case of a Gaussian distribution (which we use here), and which is closely related to the approach of Ref. 26 for the SK model.

Both in three and four dimensions, we find a tail in $P(q)$ which is independent of size (up to the sizes studied), for temperatures down to $T \simeq 0.2\, T_c$ in 3D and

$T \simeq 0.1\,T_c$ in 4D, in contrast to the prediction of Refs. 20, 21. We also find that data for the "link overlap", defined below, fits well a description with $d_s < d$, though the extrapolation to the thermodynamic limit is quite large here. Thus our results are completely consistent with the earlier proposal of KM and PY.

We consider the short-range Ising spin glass in three and four dimensions, and, in addition, the Viana-Bray[27] model. The latter is infinite range but with a finite average coordination number z, and is expected to show RSB behavior. All these models have a finite transition temperature. In the 3D case, the exponent θ obtained from the magnitude of the change of the ground state energy when the boundary conditions are changed from periodic to anti-periodic is[28] about 0.2, whereas in 4D it is much larger[29], about 0.7.

The Hamiltonian is given by

$$\mathcal{H} = -\sum_{\langle i,j \rangle} J_{ij} S_i S_j , \tag{1}$$

where, for the short range case, the sites i lie on a simple cubic lattice in dimension $d = 3$ or 4 with $N = L^d$ sites ($L \le 8$ in 3D, $L \le 5$ in 4D), $S_i = \pm 1$, and the J_{ij} are nearest-neighbor interactions chosen according to a Gaussian distribution with zero mean and standard deviation unity. Periodic boundary conditions are applied. For the Viana-Bray model each spin is connected with $z = 6$ other spins on average chosen randomly (but with the constraint that the total number of bonds is *exactly* $3N$). We allowed the local coordination to fluctuate which is different from the more familiar Viana-Bray model in which each site has exactly the same coordination number, but we expect the properties of the two models to be very similar. The width of the Gaussian distribution is again unity, and the range of sizes is $N \le 700$.

Our attention will focus primarily on two quantities: the spin overlap, q, defined by

$$q = \frac{1}{N} \sum_{i=1}^{N} S_i^{(1)} S_i^{(2)} , \tag{2}$$

where "(1)" and "(2)" refer to two copies (replicas) of the system with identical bonds, and the link overlap, q_l, defined by

$$q_l = \frac{1}{N_b} \sum_{\langle i,j \rangle} S_i^{(1)} S_j^{(1)} S_i^{(2)} S_j^{(2)} . \tag{3}$$

In the last equation, N_b is the number of bonds ($Nz/2$ for the models considered here, where z is the coordination number), and the sum is over all pairs of spins i and j which are connected by bonds. The advantage of calculating q_l as well as q is that if two spin configurations differ by flipping a large cluster then q differs from unity by an amount proportional to the *volume* of the cluster while q_l differs from unity by an amount proportional to the *surface* of the cluster.

II. EQUILIBRATION

Simulations of spin glasses at low temperatures are now possible, at least for modest sizes, using the parallel tempering Monte Carlo method[23,24]. In this technique, one simulates several identical replicas of the system at different temperatures, and, in addition to the usual local moves, one performs global moves in which the temperatures of two replicas (with adjacent temperatures) are exchanged. It turns out to be straightforward to design an algorithm which satisfies the detailed balance condition, and it will also have a good acceptance ratio if the temperatures are fairly close together. In this way, the temperature of a given replica wanders up and down in a random manner, and each time the temperature goes low the system is likely to end up in a different valley of the energy landscape. Thus different valleys are sampled in much less time than it would take for the system to fluctuate between valleys if the temperature stayed fixed.

We choose a set of temperatures $T_i, i = 1, 2, \cdots, N_T$, in order that the acceptance ratio for the global moves is satisfactory, typically greater than about 0.3. Since, at each temperature, we need two copies of the system to calculate q and q_l as shown in Eqs. (2) and (3), we actually run 2 sets of N_T replicas and perform the global moves independently in each of these two sets.

To believe results of simulations carried out at low temperatures it is essential to have a sound criterion for equilibration. The technique pioneered by Ref. 25 does not work with parallel tempering Monte Carlo because the temperature does not stay constant. However, another method can be used for a Gaussian distribution of exchange interactions, which is a common and convenient choice. It depends on an identity first noted a long time ago by Bray and Moore[30] for the SK model. Here we give the corresponding result for the short range case. We start with the expression for the average energy per site,

$$U = -\frac{1}{N} \sum_{\langle i,j \rangle} [\, J_{ij} \langle S_i S_j \rangle_T \,]_{av} , \tag{4}$$

where $\langle \cdots \rangle_T$ denotes the Monte Carlo average for a given set of bonds, and $[\cdots]_{av}$ denotes an average over the (Gaussian) bonds J_{ij}. One can perform an integration by parts over the J_{ij} to relate U to the average link overlap defined in Eq. (3), i.e.

$$\langle q_l \rangle \equiv \frac{1}{N_b} \sum_{\langle i,j \rangle} [\langle S_i S_j \rangle_T^2]_{av} = 1 - \frac{T|U|}{(z/2)J^2} , \tag{5}$$

where the brackets $\langle \cdots \rangle$ indicate both a Monte Carlo average and and an average over disorder, J^2 is the variance of the interactions (set equal to unity in this paper), the sum is over sites i and j connected by bonds (each pair counted once), and the factor of $z/2$ arises because there are $z/2$ times as many bonds as sites. A very similar approach has been used to test equilibration of the parallel tempering method for the SK model[26], except that in that case the square of the spin glass order parameter appears rather than q_l.

We start the simulation by randomly choosing the spins in the $2N_T$ replicas to be uncorrelated with each other. This means that the two sides of Eq. (5) should approach the equilibrium value from *opposite* directions for the following reason. The data for $\langle q_l \rangle$ will be too small if the system is not equilibrated because the random start means that the spins are initially further away from each other in configuration space than they will be in equilibrium, whereas initially the energy will not be as negative as in equilibrium so the right hand side of Eq. (5) will initially be too high. Hence we expect that if the two sides of Eq. (5) agree then the system is in equilibrium.

For illustration purposes we show in Fig. 1 how this works for three-dimensions with $L = 8$ and $T = 0.5$ (to be compared with[31] $T_c \simeq 0.95$). The data for $\langle q_l \rangle$ increases as the length of the simulation increases while that determined from the energy decreases (by a lesser amount). Once the two agree they do not appear to change at longer times, indicating that they have reached equilibrium, as expected. Furthermore, the data for different moments of the spin overlap q as well as the link overlap q_l appear to saturate when q_l has equilibrated so it does not appear that there are longer relaxation times for q than for q_l. We also checked that the whole distribution $P(q)$ does not change with time once the two estimates for $\langle q_l \rangle$ agree. By presenting results for an intermediate temperature, rather than the lowest temperature, in Fig. 1, we show that the results do not change for times *longer* than that needed for q_l and $1 - 2T|U|/z$ to agree. The length of the simulation was chosen so that, at *lowest* temperature, the data for q_l and $1 - 2T|U|/z$ *just converged*.

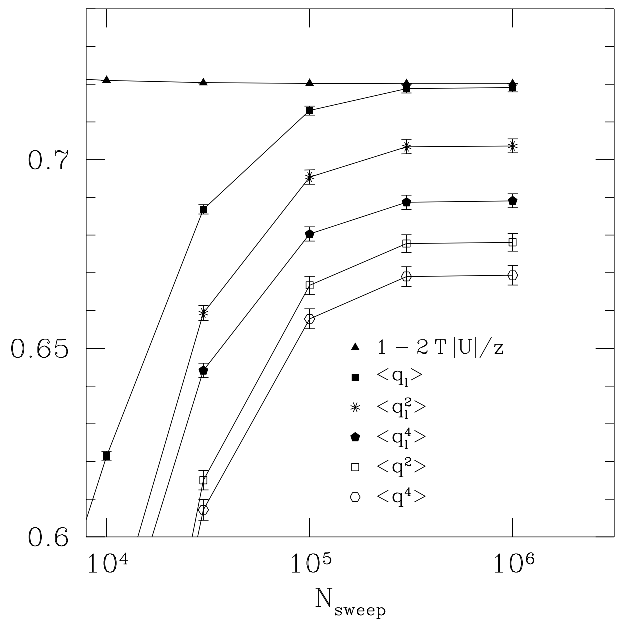

FIG. 1. The solid squares are results for the average link overlap, defined by Eq. (3), as a function of the number of Monte Carlo sweeps, N_{sweep}, that each of the $2N_T$ replicas performs. Averaging was performed over the last half of the sweeps indicated. The triangles are obtained from the energy in the way indicated, and should agree with the results for q_l if the system is in equilibrium, as shown in Eq. (5). The two sets of data approach each other from opposite directions and then do not appear to change at larger number of sweeps, indicating that they have equilibrated. We also show data for higher moments of q and q_l. They appear to be independent of the number of sweeps once the q_l data has equilibrated. The data for the different moments has been shifted upwards by the following amounts for better viewing: $\langle q^2 \rangle$ by 0.11, $\langle q^4 \rangle$ by 0.48, $\langle q_l^2 \rangle$ by 0.17, $\langle q_l^4 \rangle$ by 0.375. These results are for $d = 3, T = 0.5$ and $L = 8$, and the data is averaged over 3891 samples.

III. RESULTS

A. Three Dimensions

In Table I, we show N_{samp}, the number of samples, N_{sweep}, the total number of sweeps performed by each set of spins (replicas), and N_T, the number of temperature values, used in the 3D simulations. For each size, the largest temperature is 2.0 and the lowest temperature is 0.1. However, for $L = 8$, the data for the two lowest temperatures, $T = 0.10$ and 0.15, are not fully equilibrated so data at these temperatures has been ignored and the lowest temperature used in the analysis is 0.20. This is to be compared with[31] $T_c \approx 0.95$. The set of temperatures is determined by requiring that the acceptance ratio for global moves is satisfactory for the largest size, $L = 8$, and for simplicity the same temperatures are also used for the smaller sizes. For $L = 3, 4, 5$, and 6, the acceptance ratio for global moves is greater than about 0.6 in average and is always greater than 0.3 for each pair of temperatures. For $L = 8$ the average acceptance ratio is 0.41, and the lowest value is 0.12.

In Table II we compare the average total energy $\langle E \rangle = NU$ at $T = 0.20$ with the average ground state energy obtained by finding the ground state of each sample with a hybrid genetic algorithm, as discussed elsewhere[32]. The two energies are very close together, indicating that at this temperature our data are unlikely to be affected by the critical point.

Figs. 2 and 3 show (symmetrized) data for $P(q)$ at temperatures 0.20 and 0.50. There is clearly a peak for large q and a tail down to $q = 0$. At both temperatures one sees that the tail in the distribution is essentially independent of size. A more precise determination of the size dependence of $P(0)$ is shown in Fig. 4 where, to improve statistics, we average over the (discrete) q-values

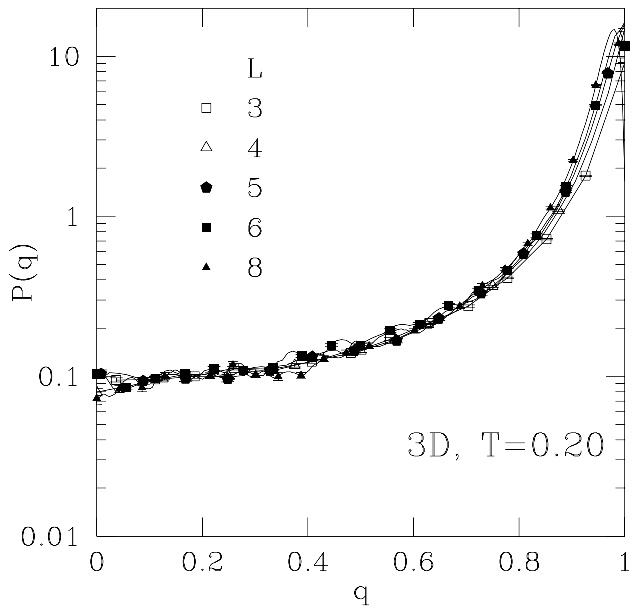

FIG. 2. Data for the overlap distribution $P(q)$ in 3D at $T = 0.20$. Note that the vertical scale is logarithmic to better make visible both the peak at large q and the tail down to $q = 0$. In this and other similar figures in the paper, we only display *some* of the data points as symbols, for clarity, but the lines connect *all* the data points. This accounts for the curvature in some of the lines in between neighboring symbols. In this paper all distributions are normalized so that the area shown under the curve is unity.

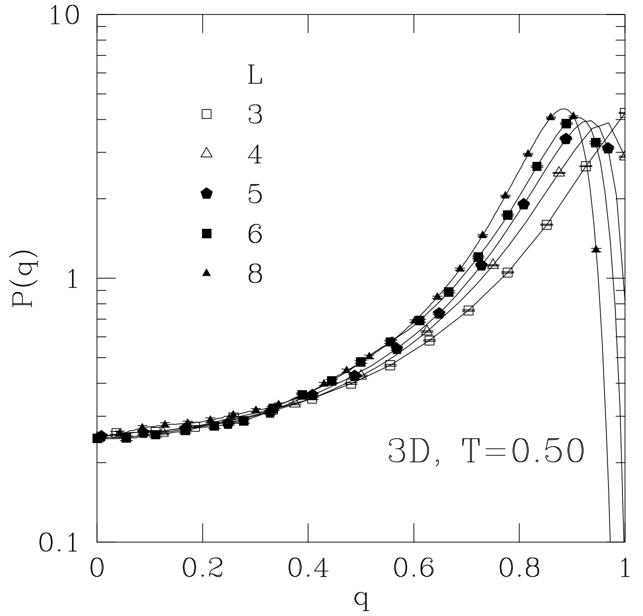

FIG. 3. Same as for Fig. 2 but at $T = 0.50$.

L	$N_{\rm samp}$	$N_{\rm sweep}$	N_T
3	15000	10^4	18
4	16000	10^4	18
5	7590	10^5	18
6	4539	3×10^5	18
8	3891	10^6	18

TABLE I. Parameters of the simulations in three dimensions. $N_{\rm samp}$ is the number of samples (i.e. sets of bonds), $N_{\rm sweep}$ is the total number of sweeps simulated for each of the $2N_T$ replicas for a single sample, and N_T is the number of temperatures used in the parallel tempering method.

L	$\langle E \rangle$	$\langle E_0 \rangle$	N_0
4	-106.49 ± 0.05	-106.60 ± 0.03	50000
6	-364.06 ± 0.17	-364.94 ± 0.06	39246
8	-867.04 ± 0.27	-868.20 ± 0.15	13302

TABLE II. Average energy $\langle E \rangle$ at $T = 0.2$ and average ground state energy $\langle E_0 \rangle$, for several sizes in three dimensions. N_0 is the number of samples used to compute the average $\langle E_0 \rangle$ using a hybrid genetic algorithm.

with $|q| < q_\circ$, with $q_\circ = 0.20$. If general, we expect that $P(0) \sim L^{-\theta'}$, where we allow θ' to be different from θ, the latter being obtained from boundary condition changes. In the droplet picture[1] $\theta' = \theta$. The dashed line in Fig. 4 has slope -0.20 corresponding to the estimated value[28] of $-\theta$, so in the droplet picture the data is expected to follow a track parallel to this line. The actual size dependence is clearly much weaker than this, and consistent with a constant $P(0)$, which implies that the energy to create a large excitation does not increase with size, and therefore $\theta' \simeq 0$.

More precisely, a two-parameter fit of the data in Fig. 4 with the form $aL^{-\theta'}$, gives $\theta' = 0.01 \pm 0.05$ for $T = 0.20$, $\theta' = 0.02 \pm 0.02$ for $T = 0.34$, and $\theta' = -0.01 \pm 0.02$, for $T = 0.50$. Different values of $q_\circ$ give similar results for the fits. We also tried a one-parameter fit in which θ' is fixed. Assuming $\theta' = 0$ the goodness-of-fit parameter Q is $0.34, 0.77$ and 0.57 for $T = 0.20, 0.34$ and 0.50 respectively, whereas assuming $\theta' = 0.20$ the goodness-of-fit parameters are very low, $1.4 \times 10^{-4}, 2.8 \times 10^{-6}$ and 7.6×10^{-15} respectively. Hence, just considering statistical errors for the sizes studied, the data is compatible with $\theta' = 0$ and not with $\theta' = 0.20$.

Refs. 20, 21 studied $P(0)$ by the Migdal-Kadanoff approximation, which is known to yield the droplet picture asymptotically. They find that, although the behavior of $P(0)$ at higher temperatures is masked by critical point effects, data at low temperatures, such as those considered here, *should* show the droplet behavior. That we find quite different results indicates that the Migdal-

Kadanoff approximation is not applicable to such small sizes. However, our data still do not rule out the possibility that the droplet theory, or some other theory, might be correct at larger sizes.

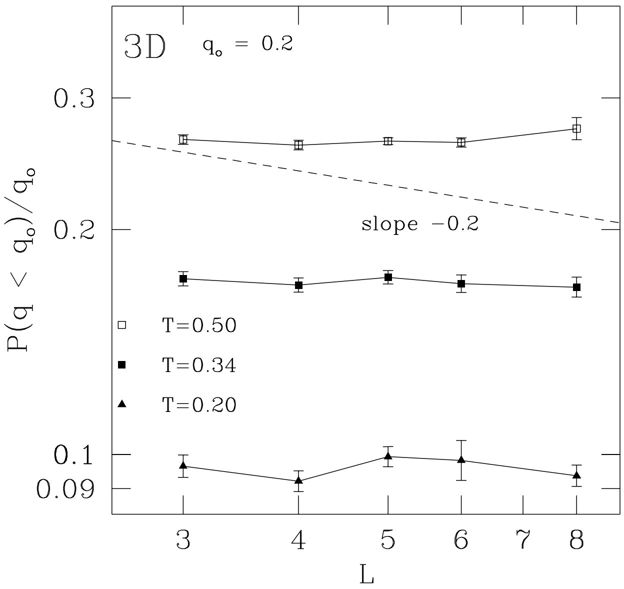

FIG. 4. Log-log plot of $P(0)$, the spin overlap at $q = 0$, against L in 3D. The data is independent of size within the error bars. The dashed line has slope −0.20, which is the estimated value of $-\theta$. Asymptotically, the data should be parallel to this line according to the droplet theory.

In Fig. 5 we show the data for $P(0)$ versus T. We see an approximately linear decrease of the data as $T \to 0$. Note though, that there is some non-linearities as shown in the figure's inset.

Fig. 6 shows the distribution of the link overlap q_l at $T = 0.20$. We see that there is a large peak at q_l close to unity (with structure coming from the allowed discrete values of q_l) and a much weaker peak (note the logarithmic vertical scale) for smaller q_l which grows slowly with increasing L and moves to larger values of q_l. We will refer to this feature again below when we discuss the Viana-Bray model.

The variance of $P(q_l)$ is shown in Fig. 8 for several low temperatures. The data is consistent with a power law decrease to zero, i.e.

$$\mathrm{Var}(\mathrm{q_l}) \sim L^{-\mu_l}, \tag{6}$$

where the power μ_l seems to vary somewhat with T. This variation is probably due to corrections to scaling coming from the shift with T of the complicated peak structure at large q seen in Fig. 6.

The asymptotic value of μ_l is related to the exponents θ' and d_s that have been mentioned earlier[33]. To see this,

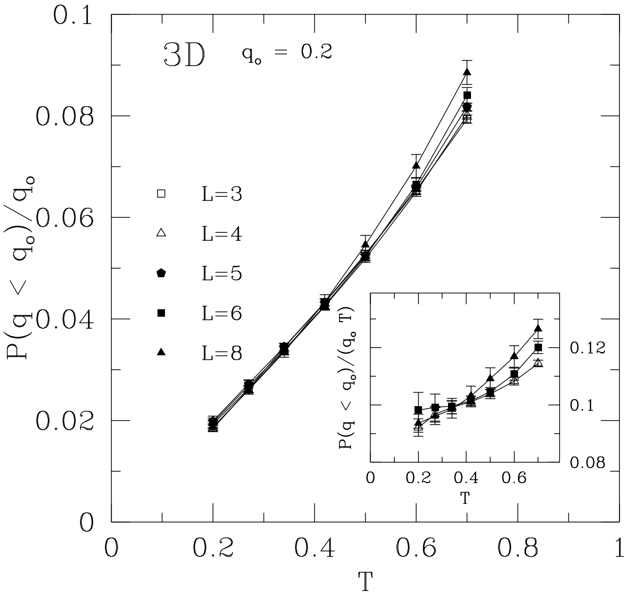

FIG. 5. Data for $P(0)$ as a function of temperature in 3D for different values of L. The inset shows $P(0)/T$ vs. T.

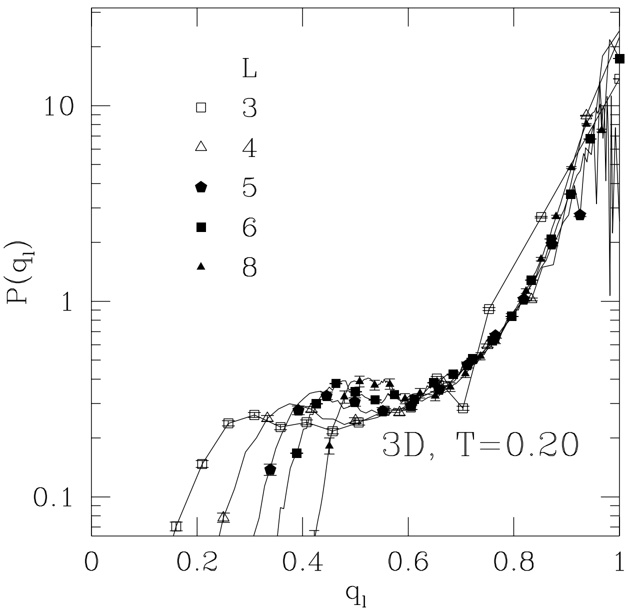

FIG. 6. The distribution of the link overlap in 3D at $T = 0.20$ for different sizes. Note the logarithmic vertical scale.

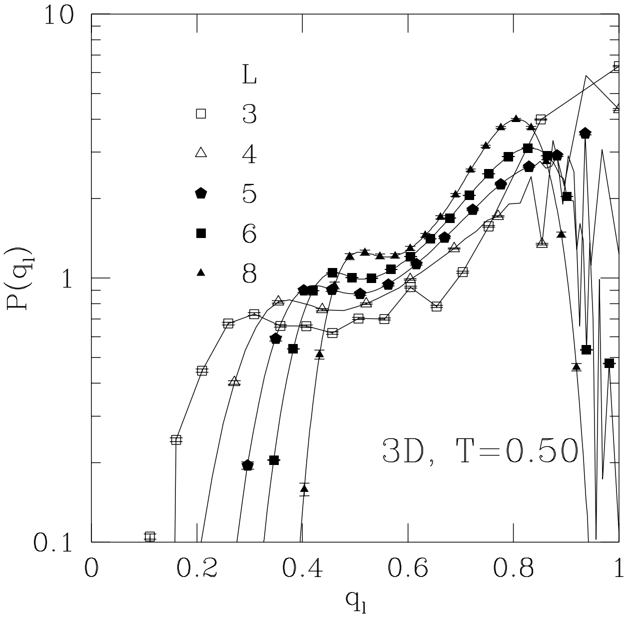

FIG. 7. Same as for Fig. 6 but at $T = 0.50$.

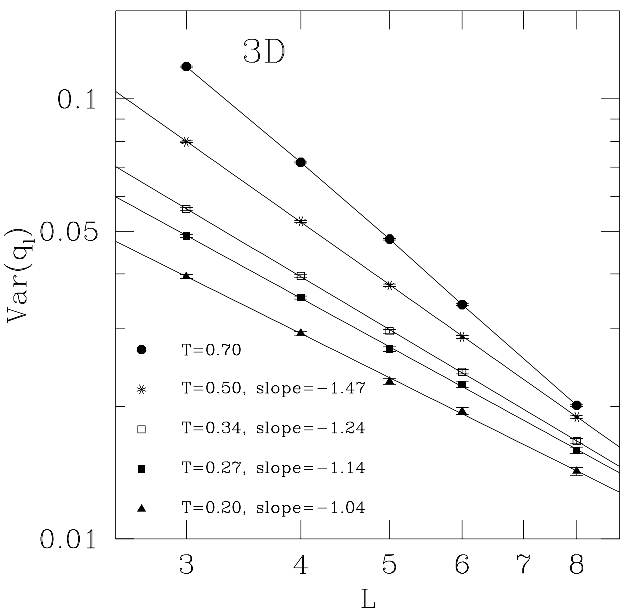

FIG. 8. Log-log plot of the variance of q_l as a function of size in 3D at several temperatures. The data for $T = 0.50$ and $T = 0.70$ are multiplied by 1.2 and 1.7 respectively for better viewing. The data for $T = 0.70$ is somewhat curved and so does not fit well a power law.

assume that the non-zero variance is largely due to the excitation of a single large cluster of size of order L. Its energy is of order $L^{\theta'}$, and the probability that thermal fluctuations can create it is of order $T/L^{\theta'}$, assuming a constant density of states for these excitations. One minus the link overlap between the two states is of order $L^{-(d-d_s)}$ because there is only a contribution to $1 - q_l$ from the surface of the cluster. Hence there is a probability $TL^{-\theta'}$ of getting a δq_l of order $L^{-(d-d_s)}$, so the variance goes like $TL^{-\mu_l}$ where

$$\mu_l = \theta' + 2(d - d_s). \tag{7}$$

An extrapolation of our results for μ_l to $T = 0$ gives 0.76 ± 0.03. Assuming $\theta' = 0$ this implies

$$d - d_s = 0.38 \pm 0.02 \tag{8}$$

which is consistent with the $T = 0$ result of PY, namely $d - d_s = 0.42 \pm 0.02$.

We have also looked at more general fits of the form

$$\mathrm{Var(q_l)} = a + \frac{b}{L^c}, \tag{9}$$

to see to what extent the data can rule out a non-zero value of a. This is of interest because a non-zero value for a is required by standard replica symmetry breaking theory. We carried out fits of the form

$$\ln[\mathrm{Var(q_l)} - a] = \ln b - c \ln L, \tag{10}$$

in which a is fixed, and $\ln b$ and c are the fit parameters. The χ^2 of the fit is then determined as a function of a and the results are shown in Fig. 9.

One sees that the minimum of χ^2 is for $a = 0$ and the range of a in which χ^2 has increased by less than unity relative to the $a = 0$ value is $a < 5.3 \times 10^{-4}$ for $T = 0.50$ and $a < 1.3 \times 10^{-3}$ for $T = 0.34$. The width of the distribution of q_l is $\sqrt{a}$ which has values 0.023 and 0.036 respectively. Thus while, our data cannot rule out a non-zero value for the width of the distribution of q_l in the thermodynamic limit, it does suggest that this value, if non-zero, must be very small. We note, however, that a rather small value of a is not unreasonable in RSB. For example, if $P(q_l)$ consists of two delta functions at a distance of 0.1, whose weights are 0.1 and 0.9 respectively, then the value of a is 0.0009.

B. Four Dimensions

In four dimensions we present results down to a temperature of 0.20, compared with[34] $T_c \approx 1.80$. Parameters of the simulations are shown in Table III. For each size, the largest temperature is 2.80 and the lowest is 0.20. The acceptance ratio for global moves is always greater than about 0.5 for $L = 3$, about 0.2 for $L = 4$ and about 0.3 for $L = 5$. In Table IV we compare the average energy at $T = 0.2$ with the average ground state energy obtained with the hybrid genetic algorithm of Ref. 32. As in 3D, the data indicate that the system is very close to the ground state.

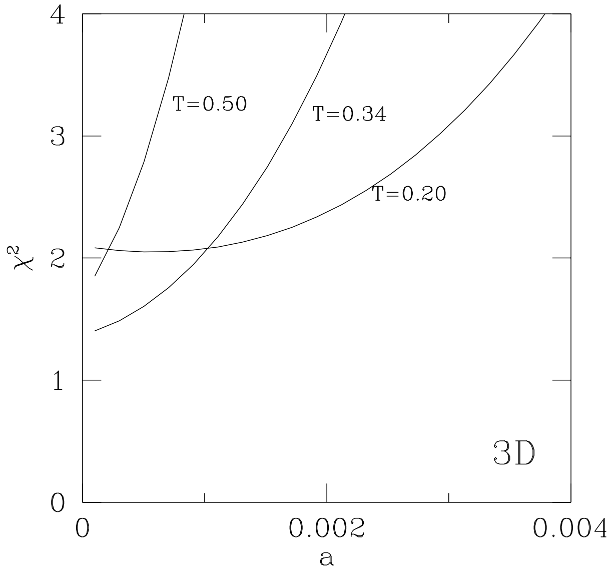

FIG. 9. The χ^2 of the fit in Eq. (10) (in which a is fixed and $\ln b$ and c are fit parameters) for different values of a. The results are for the 3D model.

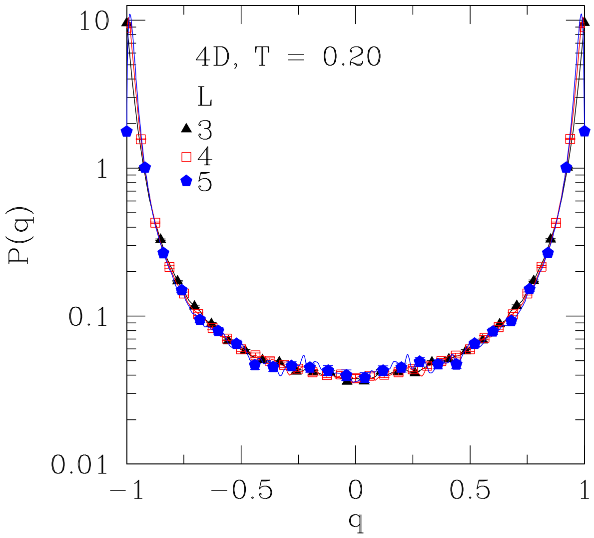

FIG. 10. Data for the overlap distribution $P(q)$ in 4D at $T = 0.20$. The data is normalized so the area under the curve is unity. Hence $P(q)$ is half as big as it it would be if we had just plotted the region of positive q as in Figs. 2 and 3.

L	$N_{\rm samp}^{(*)}$	$N_{\rm sweep}$	N_T
3	60000	6×10^3	12
4	30000	6×10^4	12
5	12190	3×10^5	23

TABLE III. Parameters of the simulations in four dimensions. $^{(*)}$ Quantities involving the link overlap q_l have been calculated with half the number of samples.

L	$\langle E \rangle$	$\langle E_0 \rangle$	N_0
3	-158.64 ± 0.03	-158.82 ± 0.04	45000
4	-510.42 ± 0.07	-510.93 ± 0.08	26681
5	-1253.41 ± 0.20	-1254.33 ± 0.20	8990

TABLE IV. Average energy $\langle E \rangle$ at $T = 0.2$ and average ground state energy $\langle E_0 \rangle$, for several sizes in four dimensions. N_0 is the number of samples used to compute the average $\langle E_0 \rangle$ using a hybrid genetic algorithm.

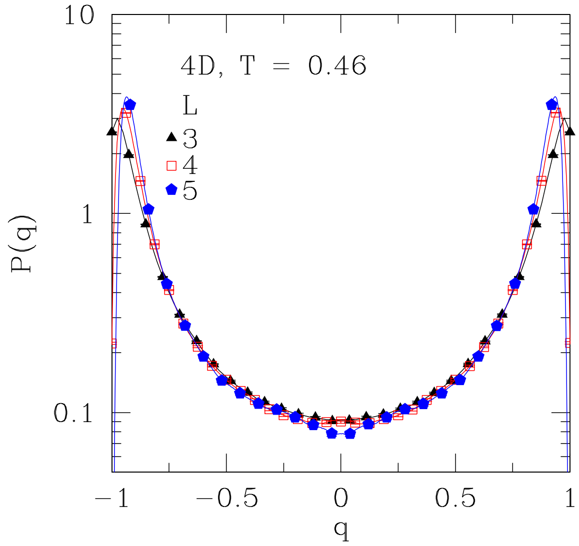

FIG. 11. Same as for Fig. 10 but at $T = 0.46$.

Figs. 10 and 11 show data for $P(q)$ for temperatures 0.20 and 0.46. As in three-dimensions, the tail in the distribution is essentially independent of size. We display the full $P(q)$, rather than just the symmetric part as in 3D, in order to show that it has a symmetric form as expected (a symmetric form was also obtained in 3D).

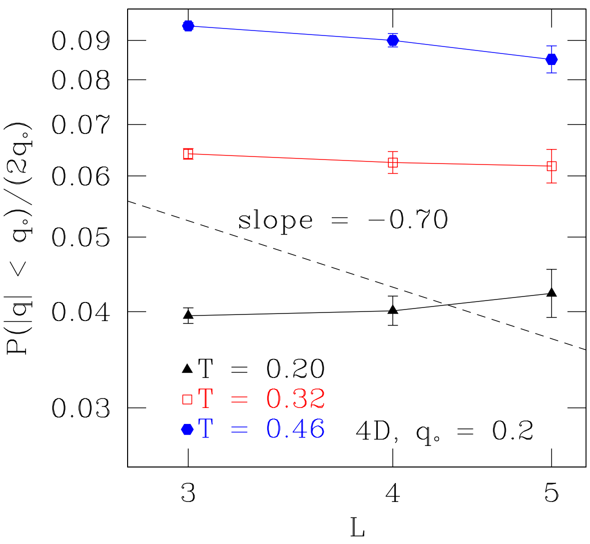

FIG. 12. Log-log plot of $P(0)$ against L in 4D averaged over the range $|q| < 0.20$. The data is independent of size within the error bars. The dashed line has slope -0.70, which is the estimated value of $-\theta$. Asymptotically, the data should be parallel to this line according to the droplet theory.

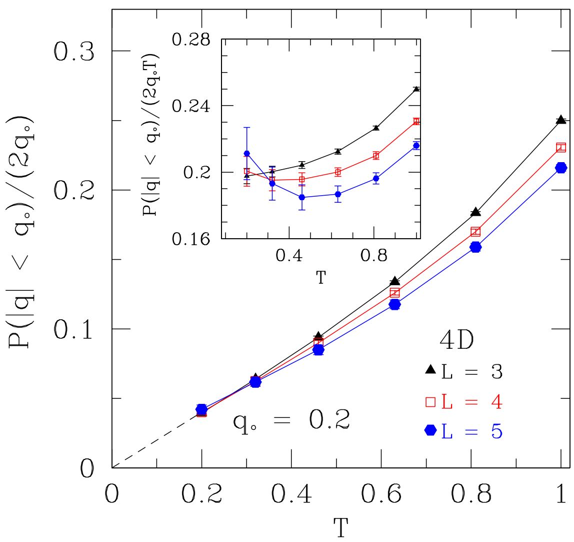

FIG. 13. Data for $P(0)$ as a function of temperature in 4D for $L = 3, 4, 5$. The inset shows $P(0)/T$ vs. T.

The size dependence of $P(0)$, averaged over the range $|q| < q_\circ$ with $q_\circ = 0.2$ is shown in Fig. 12. The dashed line has slope -0.70 corresponding to the estimated value of $-\theta$. In the droplet picture, the behavior should follow this form asymptotically. Clearly it does not for this small range of sizes. More precisely, performing a similar analysis as in 3D we find $\theta' = 0.10 \pm 0.12, 0.08 \pm 0.09$ and 0.17 ± 0.06 for $T = 0.20, 0.32$ and 0.46 respectively. For the same temperatures, the goodness-of-fit parameter is $0.67, 0.65$ and 0.014, assuming $\theta' = 0$, which is acceptable, while assuming $\theta' = 0.70$ the goodness-of-fit parameters are tiny: $2.1 \times 10^{-10}, 2.1 \times 10^{-12}$ and 4.2×10^{-18}.

As in 3D we find different results from what is predicted by Refs. 20, 21 at such low temperatures on the basis of the the Migdal-Kadanoff approximation. However, our data can not rule out the possibility that some other behavior may occur at larger sizes.

Note also, that our data for $P(0)$ decreases approximately linearly with temperature as $T \to 0$, as shown in Figure 13.

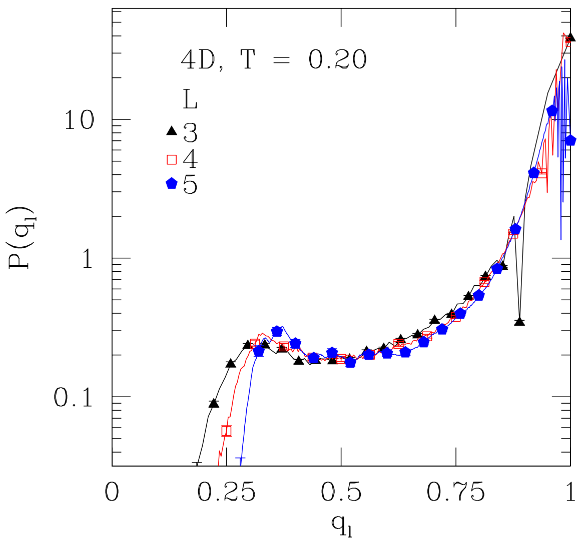

FIG. 14. The distribution of the link overlap in 4D at $T = 0.20$ for different sizes. Note the logarithmic vertical scale.

Figs. 14 and 15 show the distribution of the link overlap q_l at temperatures 0.20 and 0.46. As in 3D we see

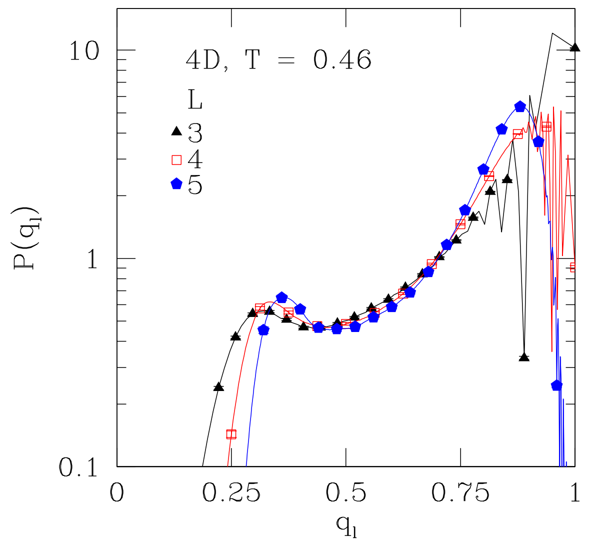

FIG. 15. Same as for Fig. 14 but at temperature 0.46.

complicated structure at large q_l and a subsidiary peak at smaller q_l which grows with increasing L.

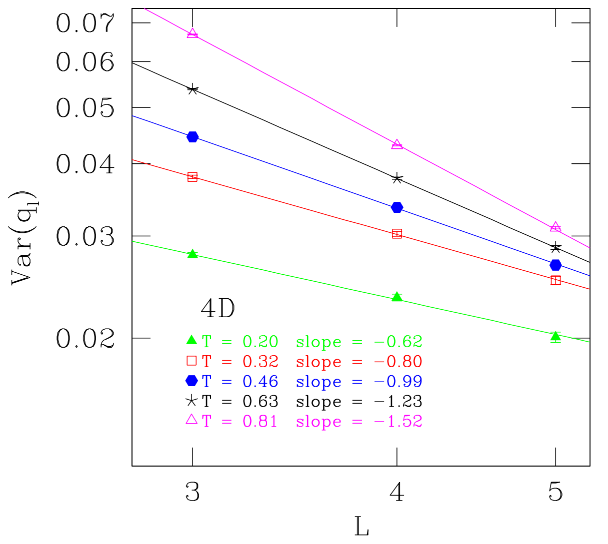

FIG. 16. Log-log plot of the variance of q_l as a function of size in 4D at several temperatures. The data for $T = 0.63$ and $T = 0.81$ are multiplied by 1.15 and 1.7 respectively for better viewing.

The variance of q_l is shown in Fig. 16 at several low temperatures. The data is consistent with the power law decrease to zero shown in Eq. (6). The range of sizes is so small, and the values of μ_l also so small, that we are not able to rule out a non-zero value for $L \to \infty$ in 4D. However, the data is *consistent* with the asymptotic value being zero.

An extrapolation of our effective values of μ_l to $T = 0$ gives 0.35 ± 0.06, which, assuming $\theta' = 0$, gives

$$d - d_s = 0.17 \pm 0.03. \tag{11}$$

This is just consistent with the $T = 0$ results of PY who find $d - d_s = 0.21 \pm 0.01$. However, the quoted error bars are from statistical errors only, so the difference may be partly due to systematic effects coming from the small range of sizes studied.

C. Viana-Bray Model

For the Viana-Bray model, T_c is given by the solution of

$$\frac{1}{\sqrt{2\pi}} \int_{-\infty}^{\infty} e^{-x^2/2} \tanh^2\left(\frac{x}{T_c}\right) dx = \frac{1}{z-1}, \tag{12}$$

where z ($= 6$ here) is the coordination number. The solution is $T_c = 1.8075\cdots$, which is roughly twice the transition temperature of the 3D short range model considered here, which has the same coordination number.

Parameters of the simulations are shown in Table V. In each case, the largest temperature is 2.6 and the lowest temperature is 0.1. For $N = 700$ the data is not equilibrated for temperatures lower than 0.34, and is almost equilibrated at $T = 0.34$. Except for $N = 700$ the acceptance ratio for global moves is always greater than about 0.3. For $N = 700$ the acceptance ratio is greater than 0.3 for most temperatures but there is one "bottleneck" where the acceptance ratio went down to 0.08.

N	$N_{\rm samp}$	$N_{\rm sweep}$	N_T
59	19022	10^4	21
99	5326	3×10^4	21
199	3116	10^5	21
399	3320	10^5	21
700	801	3×10^5	21

TABLE V. Parameters of the simulations for the Viana-Bray model.

First of all, in Fig. 17 we show that $P(q)$ has a weight at $q = 0$ which appears to be independent of the system size, as expected.

A plot of $P(q_l)$ is shown in Figs. 18 and 19 for $T = 0.34$ and 0.70. Note that the data for $N = 700$, $T = 0.34$ show a dip around $q \simeq 0.5$, due to imperfect equilibration of the Monte Carlo runs for some samples (this explains also the fluctuations of the data for $P(q)$ in Fig. 17). As in the 3D and 4D data discussed above we see a 2-peak structure develop as the size increases. This is also clearly visible in the earlier work of Ciria et al.[35] in 4D. For the Viana-Bray model, the position of the smaller peak shifts neither with L or T whereas for the 3D data, see Fig. 6, it clearly shifts to larger values of q_l with increasing size. In 4D, see Figs. 14 and 15, the range of sizes is sufficiently small that it is difficult to tell whether there is a shift in the position of the peak or not, but if it is present, it appears to be a smaller effect than in 3D. It would be helpful to understand the physics behind the two peak structure. For the hierarchical lattice used in the Migdal-Kadanoff approximation, Bokil et al.[21] have given an explanation, but it is not clear to us how this goes over to the models discussed here.

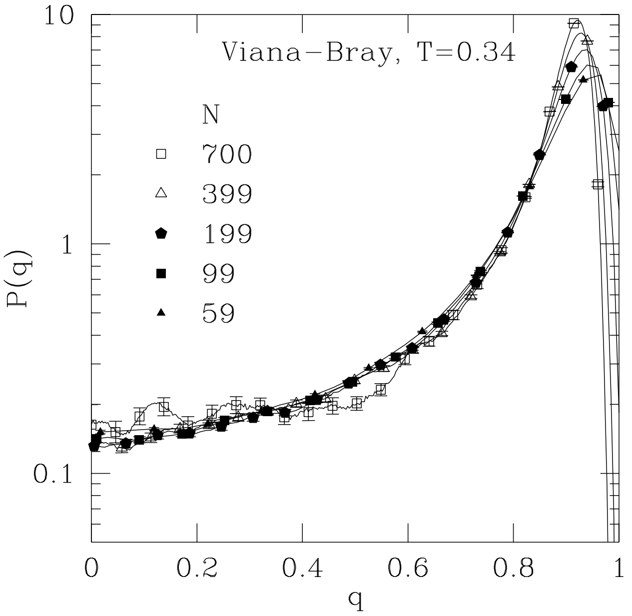

FIG. 17. Data for the distribution of the overlap for the Viana-Bray model at $T = 0.34$. Note the logarithmic vertical scale.

A plot of Var(q_l) against N is shown in Fig. 20 for different temperatures. In contrast to the data for 3D shown in Fig. 8, (which is for a similar number of spins) the data is clearly tending to a constant at large N.

This is confirmed by the χ^2 analysis of the fits corresponding to Eq. (10) shown in Fig. 21. Clearly the asymptotic value of a is large and finite. Compare this figure with Fig. 9, which shows the corresponding results in 3D, and where $a = 0$ gives the best fit.

We conclude this section by pointing out the sizes studied (which covers a similar range to that in 3D and 4D) *are* sufficient to determine the correct asymptotic behavior for the Viana-Bray model.

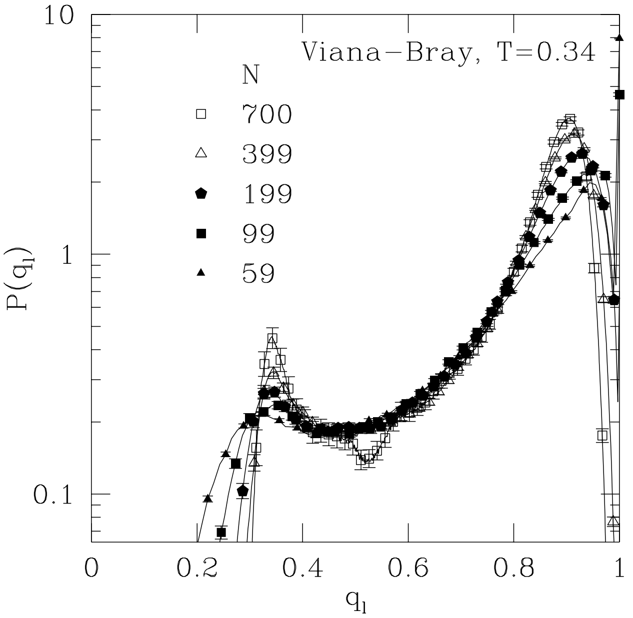

FIG. 18. Data for the distribution of the link overlap for the Viana-Bray model at $T = 0.34$. Note the logarithmic vertical scale.

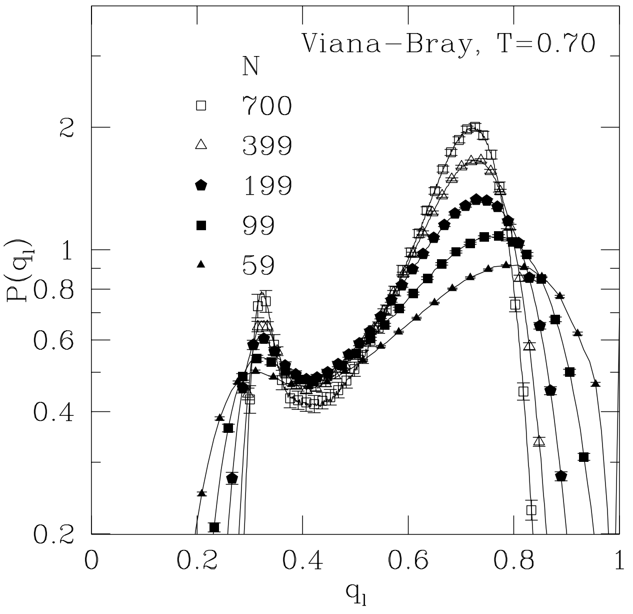

FIG. 19. Same as for Fig. 18 but for $T = 0.70$.

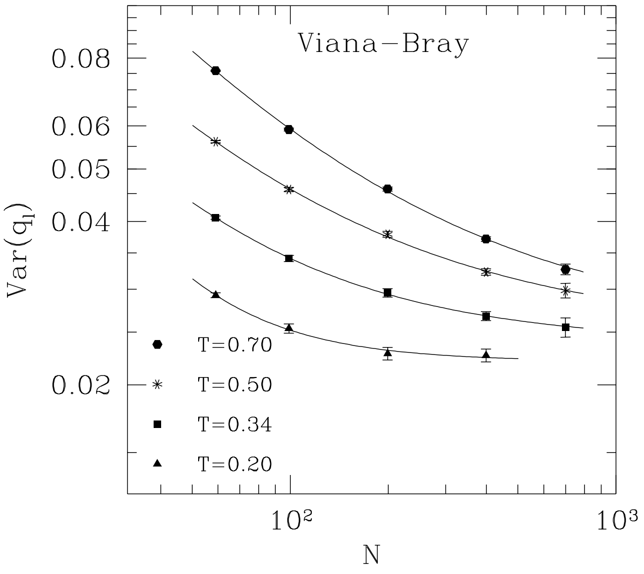

FIG. 20. A log-log plot of the variance of q_l for the Viana-Bray model at different temperatures. The data at $T = 0.5$ and $T = 0.7$ are multiplied by 1.2 and 1.6 respectively for better viewing.

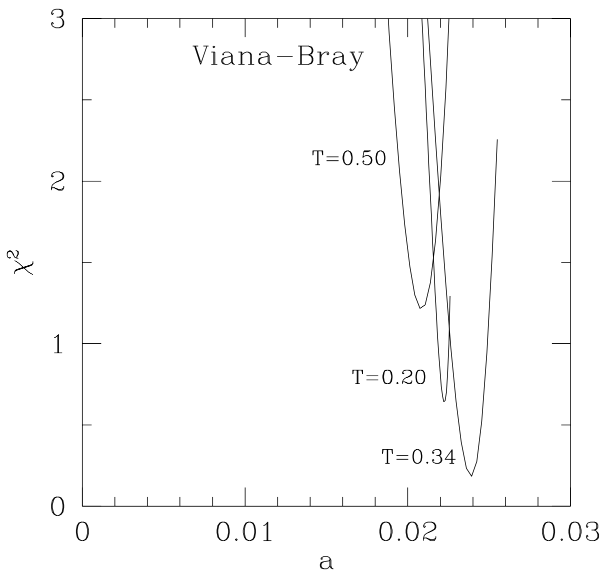

FIG. 21. The χ^2 of the fit in Eq. (10) for different values of a for the Viana-Bray model. Note that the minima of the different χ^2 are not monotonic in T since we have fewer data points for $T = 0.20$.

IV. CONCLUSIONS

To conclude, Monte Carlo simulations at low (but finite) temperatures agree with earlier $T = 0$ studies of KM and PY that there appear to be large-scale low energy excitations which cost a finite energy, and whose surface has fractal dimension less than d. However, since the sizes that we study are quite small, there could be a crossover at larger sizes to different behavior, such as the droplet theory (with $\theta' = \theta\ (> 0)$) or an RSB picture (where $\theta' = 0, d - d_s = 0$). We note, however, that our results for short range models are quite different from those of the mean-field like Viana-Bray model for samples with a similar number of spins, and, furthermore, our results for the Viana-Bray model do predict the correct asymptotic behavior for that model.

ACKNOWLEDGMENTS

We would like to thank D. S. Fisher, G. Parisi, E. Marinari, O. Martin, M. Mézard, M. A. Moore, H. Bokil and A. J. Bray for helpful discussions and correspondence. This work was supported by the National Science Foundation under grants DMR 9713977 and 0086287. The numerical calculations were made possible by a grant of time from the National Partnership for Advanced Computational Infrastructure, and by use of the UCSC Physics graduate computing cluster funded by the Department of Education Graduate Assistance in Areas of National Need program.

---

[1] D. S. Fisher and D. A. Huse, J. Phys. A. **20** L997 (1987); D. A. Huse and D. S. Fisher, J. Phys. A. **20** L1005 (1987); D. S. Fisher and D. A. Huse, Phys. Rev. B **38** 386 (1988).

[2] A. J. Bray and M. A. Moore, in *Heidelberg Colloquium on Glassy Dynamics and Optimization*, L. Van Hemmen and I. Morgenstern eds. (Springer-Verlag, Heidelberg, 1986).

[3] W. L. McMillan, J. Phys. C, **17**, 3179 (1984).

[4] G. Parisi, Phys. Rev. Lett. **43**, 1754 (1979); J. Phys. A **13**, 1101, 1887, L115 (1980; Phys. Rev. Lett. **50**, 1946 (1983).

[5] M. Mézard, G. Parisi and M. A. Virasoro, *Spin Glass Theory and Beyond* (World Scientific, Singapore, 1987).

[6] K. Binder and A. P. Young, Rev. Mod. Phys. **58** 801 (1986).

[7] C. M. Newman and D. L. Stein, Phys. Rev. B **46**, 973 (1992); Phys. Rev. Lett., **76** 515 (1996); Phys. Rev. E **57** 1356 (1998).

[8] E. Marinari, G. Parisi, F. Ricci-Tersenghi, J. Ruiz-Lorenzo and F. Zuliani, J. Stat. Phys. **98**, 973 (2000).

[9] F. Krzakala and O. C. Martin, Phys. Rev. Lett. **85**, 3013 (2000) (referred to as KM).

[10] M. Palassini and A. P. Young, Phys. Rev. Lett. **85**, 3017 (2000) (referred to as PY).

[11] E. Marinari and G. Parisi, Phys. Rev. B **62**, 11677 (2000).
[12] A. A. Middleton, cond-mat/0007375.
[13] N. Hatano and J. E. Gubernatis, cond-mat/0008115.
[14] E. Marinari, G. Parisi, F. Ricci-Tersenghi and F. Zuliani, J. Phys. A **34**, 383 (2001).
[15] M. Palassini and A. P. Young, cond-mat/0012161.
[16] G. Hed, A. K. Hartmann, E. Domany, cond-mat/0012451.
[17] J. D. Reger, R. N. Bhatt and A. P. Young, Phys. Rev. Lett. **64**, 1859 (1990).
[18] E. Marinari, G. Parisi, and J. J. Ruiz-Lorenzo, in *Spin Glasses and Random Fields*, edited by A. P. Young (World Scientific, Singapore, 1998), and references therein.
[19] E. Marinari and F. Zuliani, J. Phys. A **32**, 7447 (1999).
[20] M. A. Moore, H. Bokil and B. Drossel, Phys. Rev. Lett. **81** 4252, (1998).
[21] H. Bokil, B. Drossel and M. Moore, Phys. Rev. B **62**, 946 (2000)
[22] The basic argument of Refs. 20, 21 is that, at the critical point, $P(0)$ *increases* with L because the width of the distribution shrinks (tending to 0 for $L \to \infty$), whereas, by assumption, below T_c $P(0)$ *decreases* to zero for $L \to \infty$. Hence, for intermediate sizes and temperatures, these two effects could roughly cancel leading to a constant $P(0)$. However, in the first study of $P(q)$ below T_c, Ref. 17 found that, while $P(0)$ in 4D indeed increased with L for T just below T_c, at the lowest temperatures studied $P(0)$ initially *decreased* before leveling out, which already casts some doubt on the claim of Ref. 20, 21.
[23] K. Hukushima and K. Nemoto, J. Phys. Soc. Japan **65**, 1604 (1996).
[24] E. Marinari, *Advances in Computer Simulation*, edited by J. Kertész and Imre Kondor (Springer-Verlag, Berlin 1998), p. 50, (cond-mat/9612010).
[25] R. N. Bhatt and A. P. Young, Phys. Rev. Lett. **54**, 924 (1985); *ibid.*, Phys. Rev. B **37**, 5606 (1988).
[26] K. Hukushima, H. Takayama, and H. Yoshino, J. Phys. Soc. Japan **67**, 12 (1998).
[27] L. Viana and A. J. Bray, J. Phys. C, **18**, 3037 (1985).
[28] A. K. Hartmann, Phys. Rev. E **59**, 84 (1999). A. J. Bray and M. A. Moore, J. Phys. C, **17**, L463 (1984); W. L. McMillan, Phys. Rev. B **30**, 476 (1984).
[29] A. K. Hartmann, Phys. Rev. E **60**, 5135 (1999); K. Hukushima, Phys. Rev. E **60**, 3606 (1999).
[30] A. J. Bray and M. A. Moore, J. Phys. C, **13**, 419 (1980).
[31] E. Marinari, G. Parisi and J. J. Ruiz-Lorenzo, Phys. Rev. B, **58**, 14852 (1998).
[32] M. Palassini and A. P. Young, Phys. Rev. Lett. **83**, 5126 (1999).
[33] B. Drossel, H. Bokil, M. A. Moore and A. J. Bray, Euro. Phys. J. **B 13**, 369 (2000).
[34] G. Parisi, F. Ricci-Tersenghi and J. J. Ruiz-Lorenzo, J. Phys. A, **29**, 7943 (1996).
[35] J. C. Ciria, G. Parisi, and F. Ritort, J. Phys. A, **26**, 6731 (1993).